Applied Rheology
To appear as: Appl. Rheol. 28 (2018) 54014
DOI: 10.3933/ApplRheol-28-54014

Rheological study of poly(lactic) acid nanocomposites with carbon nanotubes and graphene additives as a tool for materials characterization for 3D printing application

Radost Ivanova and Rumiana Kotsilkova*

Open Laboratory on Experimental Micro and Nano Mechanics, Institute of Mechanics, Bulgarian Academy of Sciences, _____Street or P.O. Box Address missing, _____City and ZIP code missing, Bulgaria

* Corresponding author: kotsilkova@imbm.bas.bg

Received: 23.4.2018, Final version: 16.7.2018

Abstract:
In the last decades, one of the most critical issues concerning the control on the processing, structure and properties of nanocomposites is related to the dispersion of nanofiller in the polymer matrix and internal interactions resulting in percolation. In this study, we investigate the rheological behavior in oscillatory and steady shear flow of poly(lactic) acid based nanocomposites incorporating 0 - 12 wt% graphene nanoplates (GNP) and multi-walled carbon natotubes (OH-MWCNT). The effect of the filler contents and aspect ratio on the viscosity and viscoelastic response is evaluated. Three rheological techniques are used for estimation of rheological percolation threshold. Due to different aspect ratio and state of dispersion of GNP and MWCNTs the percolation threshold differs significantly for both compositions $\phi_p \leq 1.5$ wt% for MWCNT/PLA and $\phi_p \leq 5$ wt% for GNP/PLA. The larger the aspect ratio of nanofiller, the lower is the rheological percolation threshold. The visualized structure by TEM analysis confirms the rheological predictions for both type composites. The index of flow was estimated by the power law slope of the flow curves and a better dispersion was assumed for MWCNTs in comparison with GNPs due to the surface modification. Based on the rheological percolation threshold and the flow index, nanocomposites were classified in three groups: Newtonian, percolated composites and elastic solids. Both characteristics are used to select the printing parameters for the three groups of nanocomposites, suitable for fused deposition modeling (FDM).

Key words: carbon nanotubes, graphene nanoplates, poly(lactic)acid, viscoelastic response, rheological percolation threshold, index of flow, printing parameters.

1 *INTRODUCTION*

The polymer composites reinforced with graphene and carbon nanotubes are fastly developing research due to the ability of both nanofillers to enhance simultaneously mechanical and physical properties of nanocomposites that can widen the application of engineering polymers significantly. In order to obtain an improvement in the overall performance of the polymer matrix, the length size and shape of carbon nanofillers are usually varied and they act as reinforcing agents, when added in small amounts [1 - 9]. Some of the advantages of nanocomposites compared with conventional polymer composites are related to the enormous surface area of the nanofillers, better interactions between different phases and an efficient transmission of the load between the polymer and the filler. Moreover, graphene and carbon nanotubes have great advantages as additives in polymers for application in Additive Manufacturing (3D printing). It should be highlighted that 3D printing is not only an innovative processing technology, but it is the future of the manufacturing industries [9 - 17]. Therefore, unlimited needs exist for novel materials suitable for 3D printing for variety of applications that require improved mechanical performances, conductivity and other functional properties of the final products [12 - 17]. Nanocomposites may provide extraordinary functionality of engineering and natural polymers, this greatly expanding the ranges of applications of products resulted from additive manufacturing technologies. Due to the complexity of composition and processing, however, key issue for the mass production of such nanocomposite materials is how to gain control on the dispersion process, interactions phenomena, and processing-structure-property relations in order to obtain superior properties and good printability.

The 3D printing based on fused deposition modeling (FDM) has recently become fairly popular because it is a very cost effective technology that may produce rapidly 3D objects with a good resolution. However, this process requires melting of a thermoplastic filament prior to the additive layer to layer deposition, therefore the right thermal and rheological properties of the material is required to be used in this technology [12 - 15]. Poly(lactic) acid (PLA) polymer is extensively used for 3D printing FDM, because of easy processing, biodegradability and biocompatibility. The PLA may be reinforced with carbon-based nanomaterials to improve the

Applied Rheology
To appear as: Appl. Rheol. 28 (2018) 54014
DOI: 10.3933/ApplRheol-28-54014

strength and functionality, electrical and thermal properties of the polymer [8]. Recently, a successful development of a conductive graphene-based filament from PLA with filler loading ~14 wt.% was reported as commercially available for 3D printing application [16]. However, such high graphene loading clog the nozzle during extrusion due to aggregation of graphene sheets [12].

Rapid development of the fused deposition modeling requires fundamental understanding of the rheological behavior of novel materials that are developed for the needs of FDM 3D printing. The challenge becomes more complex with varying the filler reinforcement (e.g. nanofillers of different nature, shape and size) added to polymer due to changing of interparticle and interfacial interactions, as well as with rheological response which in turn influence the printing ability and properties of nanocomposite materials [17, 18]. Torres [17] reported that rheological measurements should be considered as a more central part of the material characterization tool when selecting suitable candidates for 3D printing. Rheology and shear rate of the material at the extrusion nozzle are used for identifying the printability window for solvent dispersions and for nanocomposite hydrogels printed via liquid deposition modeling and direct ink writing, respectively [19 - 21]. A study was published on using the rheological investigations for identifying the printability of bionanocomposites by fused deposition modeling [18].

In this article, we experimentally study the viscosity and viscoelasticity of nanocomposites based on PLA polymer incorporating graphene nanoplates (GNP) and multiwall carbon nanotubes (MWCNT), as varying the filer contents from 0 to 12 wt.%. The rheological behavior of nanocomposite melts was investigated at oscillatory and flow steady state regimes at 200°C. The contribution of graphene nanosheets with aspect ratio ~ 240 and carbon nanotubes of aspect ratio > 1000, on the viscosity and viscoelasticity of composite melts were analyzed. Three rheological criteria: Cole-Cole plot, van Gurp–Palmen plot and Power law slope of plateau modulus was used for precise estimation of the rheological percolation threshold over the experimentally studied range of nanofiller concentrations. The index of flow was related to the rheological percolation threshold in order to classify nanocomposites by their flow behavior. Both characteristics were used to identify the 3D printing parameters that ensure accuracy of the printed objects by fused deposition modeling.

2 MATERIALS AND METHODS

2.1 MATERIALS

The poly(lactic) acid (PLA) polymer used in this study was Ingeo™ Biopolymer PLA-3D850 (Nature Works) with MFR 7 - 9 g/10 min (210°C, 2.16 kg), peak melt temperature ~ 180°C, glass transition temperature ~ 60°C, tensile elongation 3.1 %. Ingeo™ 3D850 is a grade developed for manufacturing 3D printer filament having some remarkable 3D printing characteristics such as precise detail, good adhesion to build plates, less warping or urling, and low odor. The Industrial Graphene Nanoplates (GNPs) and Industrial Grade OH-Functionalized multiwall carbon nanotubes (MWCNTs) adopted as nanofillers were supplied from Times Nano, China. Their specific features are collected in Table 1. Nanocomposites of PLA polymer filled with MWCNTand GNP were prepared by melt extrusion at 180 - 190°C, using a tween screw extruder at screw speed 40 rpm, as varying the filler contents from 0 up to 12 wt.%. Further on, a filament for FDM 3D printing with diameter 1.75 mm was produced by single screw extruder at temperature 170 - 180°C and screw speed 10 rpm. Test samples of 1 mm thickness and 20 mm diameter were printed from the filaments at 200°C for rheological characterization.

2.2 EXPERIMENTAL METHODS

The rheological measurements were carried out with AR-G2 Rheometer (TA Instruments) using electrical-heated parallel plate geometry (25 mm diameter) and gap size of 500 μm between plates. The viscoelastic flow properties were measured using low amplitude oscillatory flow mode, at a temperature of 200°C. The complex dynamic viscosity η^*, storage modulus G', and loss modulus G'' were measured versus the angular frequency ω of 0.1 - 100 rad/s at low strain amplitude of 0.1 %. The linear viscoelastic strain amplitude of 0.1 % was preliminary determined by strain sweep test at angular frequency of 1 Hz. Before starting the rheological experiment, the tested material was heated at 200°C for 15 min. in the gap between the parallel plates, and pre-shear was applied to avoid unwanted errors during the measurement. The shear flow test mode was also applied and the steady-state viscosity η within the shear rate range 0.05 - 600 s^{-1} was determined, at the melt temperature 200°C. The TA Advantage Software was used for data analysis and calculation. Transmission Electron Microscope (TEM) at accelerating voltage 200 kV was used for visualization of the dispersion of GNP and MWCNTs in PLA matrix polymer. Thin slices (< 100 nm) were cut from the cross section of the filaments and visualized at different magnifications.

3 RESULTS AND DISCUSSION

3.1 CONTRIBUTION OF FILLERS TO THE VISCOELASTICITY

Applied Rheology
To appear as: Appl. Rheol. 28 (2018) 54014
DOI: 10.3933/ApplRheol-28-54014

The effect of graphene and carbon nanotubes on the linear viscoelastic response of the PLA polymer and the composites at 200°C is shown in Figure 1 and Figure 2. The frequency dependence of the dynamic complex viscosity η^* is shown in Figure 1 and the storage and loss moduli (G' & G'') versus angular frequency ω is seen on Figure 2 as varying the filler contents from 1.5 to 12 wt% for both MWCNT/PLA and GNP/PLA nanocomposites. The MWCNT/PLA composites in Figure 1a demonstrate plastic behavior of complex viscosity η^* versus angular frequency in the whole concentration range studied. In contrast, Figure 1b show that 1.5 - 6 wt% GNP/PLA composites have a Newtonian plateau in the low frequency range (ω < 10 s^{-1}), similar to the neat PLA. However, at 9 to 12 wt% GNP contents, the dynamic viscosity demonstrate plastic behavior.

In Figure 2, the viscoelastic moduli G' and G'' versus angular frequency ω show that the MWCNT/PLA composites behave differently than the GNP/PLA. In the terminal region, $\omega \rightarrow 0$, the storage G' and loss G'' modulus of the neat PLA fit with scaling law, $G' \sim \omega^2$ and $G'' \sim \omega^1$. For the MWCNT/PLA composites in Figure 2a, a solid-like viscoelastic behavior with $G' \geq G''$ is observed for the full concentration range studied from 1.5 to 12 wt%. This was associated with interconnection between nanotubes, resulting in percolation. However, for GNP/PLA composites in Figure 2b, the slope of both moduli slightly decreases by increasing the filler contents from 1.5 - 6 wt%, but the flow behavior is liquid-like with $G' < G''$. While at 9 and 12 wt% GNP, the storage modulus exceeds the loss modulus ($G' \geq G''$) and this behavior is usually related to the liquid-to-solid transition due to the formation of continuous network of graphene nanoplates in the polymer leading to retardation of the polymer chain relaxation [22 - 26]. Upon comparing the changes of the slope of $G'(\omega)$ modulus by increasing the filler contents for both composite types, we are led to assume that the more pronounced effect of carbon nanotubes on the viscoelastic response of PLA nanocomposites is probably due to both the higher aspect ratio (> 1000) and the good dispersion of OH-modified MWCNTs, compared to the dispersion of non-modified GNPs having a lower aspect ratio (~240).

3.2 CRITERIA FOR IDENTIFYING THE RHEOLOGICAL PERCOLATION THRESHOLD

It is important to determine the rheological percolation threshold as the viscosity and the properties of nanocomposites are generally enhanced above this critical filler concentration [1]. The rheological percolation threshold is usually associated with the structural liquid-to-solid transition indicating the formation of a percolation network of interconnected nanoparticles, immobilized with matrix polymer [1, 7, 22 - 24]. Different approaches are used in the literature to determine the percolation threshold [1, 23, 25]. In this study we apply three frequently used rheological criteria: Cole-Cole plot, van Gurp–Palmen plot and the power law slope of plateau modulus, in order to verify their applicability for the studied GNP/PLA and MWCNT/PLA nanocomposites for precise estimation of the rheological percolation threshold.

3.2.1 Cole-Cole plot

The first criteria used here for identifying the rheological percolation threshold is the Cole-Cole plot [26, 27], which presents the frequency dependence of imaginary viscosity η'' versus real viscosity η'. The Cole-Cole plot is used to identify the structural changes in the PLA polymer matrix due to the incorporation of fillers GNP and MWCNT. The real part and imaginary part of complex viscosity are calculated from the dynamic modulus as follows: $\eta' = G''/\omega$ and $\eta'' = G'/\omega$. Figure 3 presents the Cole–Cole plot for MWCNT/PLA and GNP/PLA composites. As seen, for the GNP/PLA composites at low nanofiller contents 0 - 3 wt%, the Cole–Cole plot exhibits a semi-circular shape with one arc corresponding to the relaxation of the PLA matrix [28]. While at 6 – 12 wt% GNP/PLA the plots exhibit deviation from the semi-circular shape and shows a linear variations of the storage viscosity versus the loss viscosity. This is a characteristic for a gel-like structure which indicates that maximum particle-particle interaction has occurred, associated with percolation. Interestingly, for MWCNT/PLA composites in Figure 3 (right), a linear plot of η'' versus η' appear at the lowest nanotube content of 1.5 wt%, thus the semi-circular shape of the Cole–Cole plot is observed only for the neat PLA. Therefore, the rheological percolation threshold that may be determined using the Cole-Cole plots is around ϕ_p < 1.5 wt% for the MWCNT/PLA composites and ϕ_p < 6 wt% for the GNP/PLA nanocomposites.

3.2.2 Van Gurp–Palmen plots

Van Gurp-Palmen (v-GP) plot of phase angle δ = tan (G''/G') versus absolute complex modulus $G^*(\omega)$ [29] is used here as the second criterion to detect the rheological percolation threshold. Figure 4 presents the v-GP plot for MWCNT/PLA and GNP/PLA nanocomposites at 200°C as varying the filler contents from 0 to 12 wt%. For the neat PLA and the GNP/PLA composites with 1.5 - 6 wt% GNP content, where the loss modulus G'' dominates over storage modulus G', the curves approach phase angle of $\delta \sim 90°$ indicating a viscous behavior. As filler contents increase to 9 wt% GNP, a significant decrease by about two orders of magnitude in the phase angle (δ < 450) at low G^* values is observed, that is ascribed for the liquid-to-solid transition [28 - 30]. While the MWCNT/PLA com-

Applied Rheology
To appear as: Appl. Rheol. 28 (2018) 54014
DOI: 10.3933/ApplRheol-28-54014

posites filled with 1.5 - 3 wt% demonstrate very low phase angle ($\delta \sim 30$ - 200) indicating liquid-to-solid transition. Moreover, at nanotube contents of 6 - 12 wt% an equilibrium modulus indicating that *G'* is over *G"* which can be determined by extrapolating the van Gurp–Palmen plot curves to $\delta = 0°$. Thus, the rheological percolation threshold is determined below $\phi_p < 1.5$ wt.% for MWCNT/PLA composites, while the GNP/PLA composites have percolation above $\phi_p > 6$ wt.% as determined by v-GP criteria.

3.2.3 *Concentration dependence of plateau storage modulus*

The third criteria used herewith for determination of rheological percolation threshold is the concentration dependence of the dynamic storage modulus that may identify the liquid-to-solid transition, related to percolation. The Figure 5 compares the storage modulus at a low frequency G_o' at $\omega = 0.1$ rad/s versus the nanoparticle loading ϕ wt% for GNP/PLA and MWCNT/PLA nanocomposites. The critical concentration ϕ_p that is the starting point for the appearance of the scaling law, $G_o' \sim \phi^n$ was determined and referred as the rheological percolation threshold [24]. As seen from Figure 5, the rheological percolation threshold differs for the two nanocomposite types, due to different shape, aspect ratio and state of dispersion of the GNP and MWCNT nanoparticles in the PLA matrix polymer. The slope of $G_o'(\phi)$, related to percolation was identified below the $\phi_p < 1.5$ wt% for the MWCNT/PLA composites. Importantly, this criterion allows determining more precisely the rheological percolation threshold for the GNP/PLA composites ($\phi_p \geq 5$ wt% GNP) as the cross point of the two power law slops of $G'(\phi)$ over the experimentally studied range of nanofiller concentrations. While the Cole-Cole plot and van Gurp–Palmen plot determine this percolation threshold with some variations, below and higher of 6 wt% GNP, respectively. Obviously, the larger aspect ratio (> 1000) and better dispersion of OH-modified MWCNTs contribute to the network formation at lower filler content of nanotubes in the PLA matrix, this resulting in a low percolation threshold of $\phi_p \leq 1.5$ wt% PLA/MWCNT. In contrast, the smaller aspect ratio (> 240) and not well dispersed GNP nanoplates in the PLA matrix lead to high percolation threshold of $\phi_p \approx 5$ wt% of GMP/PLA.

3.3 *VISUALIZATION OF NANOFILLER DISPERSION IN NANOCOMPOSITES*

In order to visualize the nanofiller dispersion in the PLA matrix we have performed transmission electron microscopy of the cross section of the filaments, produced from the nanocomposites studied. Figure 6 presents example TEM images of 6 wt% MWCNT/PLA and 6 wt% GNP/PLA composites at high and low magnifications. We compare composites with the same filler content of 6 wt%, around and above the percolation threshold, determined above, in order to compare the size of nanocarbon fillers, as well as their dispersion and structure in the polymer. As seen on Figure 6a at high magnifications, the MWCNTs are uniformly dispersed in the PLA matrix and their visible average length is of ~ 200 nm. Therefore the MWCNTs in the composite have much lower length in comparison with the commercial filler before mixing with the polymer, according to the technical specification from the producer (Table 1). At low magnification (Figure 6c) the homogeneous dispersion of MWCNTs in the PLA matrix is more clearly presented. It is visible that nanotubes of different length fill the whole volume of the polymer and they form a network of contacting particles, associated with percolation. The visualized in Figure 6a and 6c structure of interconnected MWCNT nanotubes in the PLA matrix confirm the rheologically determined solid-like behavior (or gel-like structure), highly above the percolation threshold for the 6 wt% MWCNT/PLA nanocomposites. In contrast, separate and large GNP nanoplates of mean size about 200 - 400 nm and thickness above 30 nm are visible in Figure 6b at high magnification. But, at low magnification (Figure 6d), it is seen that graphene nanoplates are partly dispersed to thinner sheets, but most of GNP are visible as thick and large aggregates of length 5 - 7 μm, similar to the original size of GNP before mixing with PLA (Table 1). The graphene sheets seems to be partly connected in the volume of nanocomposite, as shown in Figure 6d, and this confirm the predicted in Figures 3 - 5 structure around percolation threshold of the 6 wt.% GNP nanocomposite.

3.4 *FLOW INDEX AND PRINTING PARAMETERS*

3.4.1 *Flow index*

The flow behavior of nanocomposite formulations in steady-state shear mode was studied as varying the filler contents from 0 to 12 wt%. Figure 7 presents the shear flow curves, i.e. viscosity η versus shear rate $\dot{\gamma}$ in a wide shear rate range 0.05 - 600 s^{-1} at a melt temperature of 200°C for GNP/PLA and MWCNT/PLA nanocomposites, respectively. The experimental data of the viscosity at low shear rates ($\dot{\gamma} < 10\ s^{-1}$) were fit with the power-law fluid model Equation 1 in order to determine the power law slop called "flow index' [1]

$$\eta = K\dot{\gamma}^{n-1} \quad (1)$$

Applied Rheology
To appear as: Appl. Rheol. 28 (2018) 54014
DOI: 10.3933/ApplRheol-28-54014

where η is the steady-state viscosity [Pas], $\dot{\gamma}$ the shear rate [s^{-1}], K the flow consistency index at ($\dot{\gamma} \rightarrow 0$), and the power-law slope n is the flow index. If we consider the low shear rates region, $\dot{\gamma} < 10\ s^{-1}$, the viscosity of the neat PLA (Figure 7) show a Newtonian plateau with $n \approx 1$. In Figure 7a, the 1.5 - 3 wt% GNP/PLA composites show plateau behavior similar to the neat PLA with $n \sim 1$. The n values started to decrease around and above 6 wt% GNP, but only 9 - 12 wt% PLA composites show low slope values ($n < 0.5$). Theoretically, the slope value of $n \leq 0.5$ for composites is usually associated with liquid-to-solid transition, which relates to percolation [28]. This confirms the percolation threshold of $\phi_p \geq 5$ wt% GNP/PLA, identified above. In contrast, in Figure 7b the lowest filler content of 1.5 wt% MWCNT/PLA nanocomposites demonstrate the slope value $n = 0.515$, that is typical for percolated composites. By increasing the filler contents to 12 wt% MWCNTs, the slope decreases significantly. The results confirm the percolation threshold of $\phi_p \leq 1.5$ wt% MWCNTs/PLA identified above. The lower slope values n at the same filler content for the MWCNT/PLA composites, compared to the slope values of GNP/PLA composites, is associated with the higher aspect ratio and batter dispersion of OH-modified MWCNTs in the PLA matrix, compared to the GNP nanofiller. Based on the values of the flow index n of the nanocomposite melts, we classify three types of nanocomposite structures, depending on the GNP and MWCNT contents and the percolation threshold ϕ_p such as: (i) Newtonian composites for $1 > n > 0.5$ (at filler contents below ϕ_p), (ii) percolated composites for $0.5 > n > 0.2$ (at filler contents around ϕ_p), and (iii) elastic solidsfor $0.2 > n > 0$ (at filler contents highly above ϕ_p).

3.4.2 *Printing parameters*

The high shear rates region ($\dot{\gamma} > 100\ s^{-1}$) in Figures 6a nd 6b is of interests for 3D printing by fused deposition modeling (FDM), where the layer to layer deposition is performed by flow of polymer melt through a nozzle. The shear rate at the nozzle wall can be described by Equation 2 [20, 31]:

$$\dot{\gamma}_{wall} = \frac{4Q}{\pi R^3}\left(\frac{3n+1}{4n}\right) = \frac{4V}{R}\left(\frac{3n+1}{4n}\right) \quad (2)$$

where γ_{wall} is the wall shear rate [s^{-1}], Q the volumetric flow rate [mm^3/s], V the average fluid velocity [mm/s], R the nozzle radius [mm], and n the flow index. Then, the printing velocity,V can be related to the wall shear rate $\dot{\gamma}_{wall}$ by the Equation 3:

$$V = \frac{R\dot{\gamma}_{wall}}{4} \quad (3)$$

In FDM applications, the printing parameters refers to the applied printing velocity V, which is necessary to achieve appropriate volumetric flow rate Q of the melt out of the nozzle with definite diameter, that will ensure accuracy of the resulting printed object. In order to ensure the same accuracy of printing for the neat PLA and the composites, we need to have the same volume of flowing material from the nozzle. Therefore, we need of a constant volumetric flow rate (Q = const.) during printing with the neat PLA and the composites. Based on this, by using upper equations (Equations 2 and 3) we define the FDM printing parameters for the neat PLA and the composites as varying the GNP and MWCNT contents at a fixed melt temperature. In Table 2 we present the relation between the flow index n of the printing material and the printing speed V, at a constant volumetric flow rate Q. The Q value is determined by Equation 1 for the neat PLA (with flow index $n = 1$) for a definite printing speed V_{PLA}, nozzle radius R, and printing temperature T. If we need to have the same volumetric flow rate Q for the composites as that for the neat PLA, the printing speed V_{comp} has to increase for the composite materials with flow index ($n < 1$), as calculated from Eqs. (1 and 2). Moreover, the increase of V_{comp} is strongly dependent from the filler content and the filler type, that is determined by the n values around and above the percolation threshold ϕ_p. In Table 2 we show the calculated by Equations 1 and 2 limits of the Vcomp increase correlated with the n values for the three nanocomposite types, i.e Newtonian, percolated, and elastic solids.

To prove the concept, we consider the FDM 3D printer German RepRap X400 having printing speed limits of V = 10 - 200 mm/s. For 3D printing of the neat PLA material we choose the following printing parameters: printing temperature 200°C, nozzle diameter d = 0.5 mm, and printing speed V_{PLA} = 10 mm/s. The calculated volumetric flow rate Q for the neat PLA is $Q = 2\ mm^3/s$ at these printing conditions. If fix the same volumetric flow rate $Q = 2\ mm^3/s$ for the composites too, we calculate the printing velocity V_{comp} for all studied PLA composites

Applied Rheology
To appear as: Appl. Rheol. 28 (2018) 54014
DOI: 10.3933/ApplRheol-28-54014

as varying the contents of the GNP and MWCNTs and the respective flow index n by using Equations 2 and 3. Table 3 summarizes the values of the wall shear rate $\dot{\gamma}_{wall}$ and printing velocity V at Q = 2 mm³/s, for the neat PLA compared to the MWCNT/PLA and GNP/PLA nanocomposites correlated with the flow index n of the respective materials.

As seen, the calculated printing speed of the Newtonian composites is similar to that of the neat PLA. However, for percolated composites the printing speed increases about $V_{comp} \sim (1.5 - 2)V_{PLA}$, while for the elastic solids this increase is much stronger, i.e. $V_{comp} \sim (2.4 - 4.3)V_{PLA}$. The results confirm the proposed in Table 2 increase of the printing speed depending on the index of flow. Arrows in Figures 7a and 7b show the printing shear rate of the neat PLA and 12 wt% composites filled with GNP and MWCNTs. Therefore, the printing of the PLA based nanocomposite materials with GNP and MWCNTs can be accomplished, if the appropriate combinations of processing conditions are employed, this including: (i) Constant volumetric flow rate during printing determined for the neat polymer and used also for the composites, as well as (ii) printing speed has to increase in correlation with the flow index n of the material. Both are determined for the same temperature and nozzle diameter. The results in Table 3 are validated by direct printing of objects using the filament (1.75 mm of diameter), produced by single screw extruder from the neat PLA and the MWCNT/PLA and GNP/PLA nanocomposite formulations, as varying filler contents within 0 - 12 wt%. The printing is performed with 3D printer German Rep Rap X-400 PRO at 200°C, with nozzle diameter 0.5 mm and melt temperature of 200°C. The volumetric velocity was fixed to Q = 2 mm³/s for all types of materials studied, by varying the printing speed from 10 to 43 mm/s, depending on the flow index n of the material, according to Table 3. Figure 8 presents example printed samples for thermal conductivity tests, with printing density 100 %, produced by these printing conditions. We found that small samples are printed with the same accuracy from both the neat PLA and the filled composites within the filler contents range (1.5 - 12 wt%). For large size details, that requires long time of printing (> 2 h) clog the nozzle during extrusion may appear when using composite filaments with 9 and 12 wt% MWCNTs (i.e. elastic solids with very low values of flow index $n \leq 0.1$). This obviously due to the large agglomerates formed by entangled nanotubes in the elastic solid composites.

Studies on the properties of 3D printed samples from GNP/PLA and MWCNT/PLA filaments with filler contents varying from 1.5 to 12 wt.% were performed in order to investigate the enhancement of electrical, electromagnetic, thermal and mechanical properties, around and above the percolation threshold [33 - 35]. The obtained results confirm that above the percolation threshold the material started to be conductive in DC [32, 33], as well as the imaginary part of dielectric permittivity is enhanced. The MWCNT/PLA composites are more conductive than the GNP/PLA at the same filler content. Moreover, the hardness and elastic modulus are significantly improved above the percolation threshold for the MWCNT/PLA nanocomposites, but such effect is not pronounced for the GNP/PLA nanocomposites [34]. The thermal conductivity gradually increases in 3D printed carbon-based PLA nanocomposites by increasing the nanocarbon content [35]. It was found that graphene nanoplates at 12 wt% content increase the thermal conductivity about 265 % compared to the neat resin and an increase of about 82 % was observed for the MWCNT/PLA composites at the same filler content. Therefore, of strong interest is to ensure the possibility for printing of objects with high accuracy using materials with filler contents above the percolation threshold (e.g. percolated composites and elastic solids).

4 CONCLUSIONS

Characterization of rheological properties of PLA nanocomposites filled with graphene nanoplates (GNP) and multiwall carbon nanotubes (MWCNT) was performed in oscillatory and shear flow mode as varying the nanofiller content from 0 to 12 wt%, at melt temperature of 200°C. The effect of aspect ratio of GNP (240) and MWCNT (1000) as well as the nanofiller dispersion was assessed by the power law slope of the storage modulus versus frequency, as well as the slope of shear viscosity versus shear rate curves. The addition of both nanofillers to PLA matrix enhance the values of the dynamic moduli at low frequencies and decrease the slope, however this effect is more pronounced for the multiwall carbon nanotubes, due to the higher aspect ratio and better dispersion of OH modifier MWCNTs, compared to the non-modified GNP with lower aspect ratio. Three rheological criteria were applied for determining the liquid-to-solid transition, associated with rheological percolation threshold ϕ_p such as: Cole-Cole plot, van Gurp–Palmen plot, and power law slope of $G_o' \sim \omega^n$. The last criterion allows determining more precisely the rheological percolation threshold, thus ϕ_p < 1.5 wt% MWCNTs and $\phi_p \sim$ 5 wt% GNP were determined for both composites. Both, rheological percolation threshold and flow index determined from the steady-state shear viscosity were used to classify three structural nanocomposite types in the wide range of filler concentrations such as: Newtonian type ($n \sim 1$, below percolation threshold), percolated composites ($0.5 > n > 0.2$ at filler contents around percolation threshold), and elastic solids ($n << 0.2$,at filler contents highly above the percolation threshold).

To appear as: Appl. Rheol. 28 (2018) 54014
DOI: 10.3933/ApplRheol-28-54014

In order to achieve a good accuracy of the printing objects, the printing of the neat PLA and the nanocomposite systems with GNP and MWCNTs was accomplished at appropriate conditions, including: (i) Constant volumetric flow rate *Q* for the neat polymer and the composites, and (ii) the printing speed *V* is increased in correlation with the flow index *n* of the printed material. These characteristics are determined for the fixed melt temperature and nozzle diameter. The concept was validated by direct printing of samples for thermal and mechanical tests, using the filament from the neat PLA, the MWCNT/PLA and GNP/PLA nanocomposite formulations studied. Small samples are printed with a good accuracy.

ACKNOWLEDGEMENTS

This work was carried out within the framework of the H2020-MSCA-RISE-2016-734164 Graphene 3D. Part of research is supported by H2020-SGA-FET-GRAPHENE-2017-785219 Graphene Core2. Authors thank Dr. Evgeni Ivanov (IMech-BAS) and Dr. Clara Silvestre (IPCB, CNR, Italy) for providing the nanocomposite materials. Dr. Dzhihan Menseidov (IMech-BAS) is acknowledged for the 3D printing of nanocomposite specimens.

REFERENCES

[1] Kotsilkova R: Thermosetting nanocomposites for engineering application, Rapra Smiths Group, UK (2007).
[2] Chee WK, Lim HN, Huang NM, Harrison I: Nanocomposites of graphene/ polymers: A review. RSC Adv. 5 (2015) 68014 - 68051.
[3] Tjong SC: Polymer Composites with Carbonaceous Nanofillers: Properties and Applications, Wiley-VCH (2012).
[4] Papageorgiou DG, Kinloch IA, Young RJ: Graphene/elastomer nanocomposites, Carbon 95 (2015) 460 - 484.
[5] Shen MY, Chang TY, Hsieh TH, Li YL, Chiang CL, Yang H, Yip MC: Mechanical properties and tensile fatigue of graphene nanoplatelets reinforced polymer nanocomposites, J. Nanomat. (2013) 565401,
[6] Kotsilkova R, Ivanov E, Krusteva E, Silvestre C, Cimmino S, Duraccio D: Isotactic polypropylene composites reinforced with multiwall carbon nanotubes. Part. 2. Thermal and mechanical properties related to the structure, J. Appl. Polym. Sci. 115 (2010) 3576 - 3585.
[7] Kotsilkova R, Ivanov E, Krusteva E, Silvestre C, Cimmino S, Durracio D: Evolution of rheology, structure, and properties around the rheological flocculation and percolation thresholds in polymer nanocomposites, in Ecosustainable Polymer Nanomaterials for Food Packaging, Silvestre C and Cimmino S (Eds), Taylor & Francis Books (2013).
[8] Gonçalves C, Gonçalves I.C, Magalhães FD, Pinto AM: Poly(lactic acid) composites containing carbon-based nanomaterials: A review, Polymers 9 (2017) 269.
[9] Ivanov E, Velichkova H, Kotsilkova R, Bistarelli S, Cataldo A, Micciulla F, Bellucci S: Rheological behavior of graphene/epoxy nanodispersions, Appl. Rheol. 27 (2017) 24469.
[10] Kotsilkova R, Ivanov E: Optimization of flow behaviour of nanodispersions by additives: Carbon and ketjen black nanoparticles in acrylic resin, in Nanoscience & Nanotechnology, Balabanova E and Dragieva I (Eds.), Heron Press (2004).
[11] Dhar P, Ansari MHD, Gupta SS, Siva VM, Pradeep T, Pattamatta A, Das SK: Percolation network dynamicity and sheet dynamics governed viscous behavior of polydispersed graphene nanosheet suspensions, J. Nanopart. Res. 15 (2013) 2095.
[12] Bustillos J, Montero D, Nautiyal P, Loganathan A, Boesl B, Agarwal A: Integration of graphene in poly(lactic) acid by 3D printing to develop creep and wear-resistant hierarchical nanocomposites, Polym. Compos. _____ Volume missing (2017) 1 - 12_____Please also check page number.
[13] Gnanasekaran K, Heijmans T, van Bennekom S, Woldhuis H, Wijnia S, de With G, Friedrich H: 3D printing of CNT- and graphene-based conductive polymer nanocomposites by fused deposition modeling, Appl. Mater. Today 9 (2017) 21 – 28.
[14] Kwok SW, Goh KHH, Tan ZD, Tan STM, Tjiu WW, Soh JY, Ng ZJG, Chan YZ, Hui HK, Goh KE J: Electrically conductive filament for 3D-printed circuits and sensors, Appl. Mater. Today 9 (2017) 167 - 175.
[15] Sanatgar RH, Campagne Ch, Nierstrasz V: Investigation of the adhesion properties of direct 3D printing of polymers and nanocomposites on textiles: Effect of FDM printing process parameters, Appl. Surf. Sci. 403 (2017) 551 - 563.
[16] Graphene 3D Lab Inc: 3D, BlackMagic. Conductive graphene filament (Msds), _____Please check for correct title, Graphene 3D Lab Inc. (2015).
[17] Torres MD: Role of the rheology in the new emerging technologies as 3D printing, Rheol. 1 (2017) e103.
[18] Aho J, Boetker JP, Baldursdottir S, Rantanen J: Rheology as a tool for evaluation of melt processability of innovative dosage forms, Int. J. Pharma. 494 (2015) 623 - 642.
[19] M'Barki A, Bocquet L, Stevenson A: Linking rheology and printability for dense and strong ceramics by direct ink writing, Sci. Rep. 7 (2017) 6017_____Check for correct manuscript number.
[20] Postiglione G, Natale G, Griffini G, Levi M, Turri S: Conductive 3D microstructures by direct 3D printing of polymer/carbon nanotube nano-composites via liquid deposition modeling, Composites A 76 (2015) 110 - 114.
[21] Li H, Liu S, Li L: Rheological study on 3D printability of alginate hydrogel and effect of graphene oxide, Int. J. Bioprint. 2 (2016) 54 - 66.
[22] Chatterjee T, Krishnamoorti R: Rheology of polymer carbon nanotube composites, Soft Matter 9 (2013) 9515 - 9529.
[23] Hassanabadi HM, Wilhelm M, Rodrigue D: A rheological criterion to determine the percolation threshold in polymer nano-composites, Rheol. Acta 53 (2014) 869 - 882.
[24] Buscall R, Mills PDA, Goodwin JW, Lawson DW: Scaling behavior of the rheology of aggregate network formed by colloidal particles, J. Chem. Soc. Faraday Trans. 84 (1998) 4249 - 4260.

To appear as: Appl. Rheol. 28 (2018) 54014
DOI: 10.3933/ApplRheol-28-54014

[25] Wu D, Wu L, Zhou W, Sun Y, Zhang M: Relations between the aspect ratio of carbon nanotubes and the formation of percolation networks in biodegradable polylactide/carbon nanotube composites, J. Polym. Sci. B 48 (2010) 479 - 489.
[26] Kalathi JT, Grest GS, Kumar SK: Universal viscosity behavior of polymer nano-composites, Phys. Rev. Lett. 109 (2012) 198301.
[27] Kiss A, Fekete E, Pukanszky B: Aggregation of $CaCO_3$ particles in pp composites: Effect of surface coating, Compos. Sci. Technol. 67 (2007) 1574 - 1583.
[28] Wu D, Wu L, Zhang M: Rheology of multi-walled carbon nanotube/poly(butylene terephthalate) composites, J. Polym. Sci. B 45 (2007) 2239 - 2251.
[29] Van Gurp M, Palmen J: Time-temperature superposition for polymer blends, Rheol. Bull. 67 (1998) 5 - 8.
[30] Yihu Song Y, Zheng Q: Linear rheology of nanofilled polymers, J. Rheol. 59 (2015) 155 - _____final page number missing.
[31] Bruneaux J., Therriault D, Heuzey M-C: Micro-extrusion of organic inks for direct-write assembly, J. Micromech. Microeng. 18 (2008) 115020.
[32] Bychanok D, Angelova P, Paddubskaya A, Meisak D, Shashkova E, Demidenko M, Plyushch A, Ivanov E, Krastev R, Kotsilkova R, Ogrin FY, Kuzhir P: Terahertz absorption in graphite nanoplatelets/polylactic acid composites, J. Phys. D 51 (2018) 145307.
[33] Spinelli G, Lamberti P, Tucci V, Ivanova R, Tabakova S, Ivanov E, Kotsilkova R, Cimmino S, Di Maio R, Silvestre C: Rheological and electrical behaviour of nanocarbon/poly(lactic) acid for 3D printing applications, Composites B, 2018 (submitted)_____any update available?
[34] Kotsilkova R, Ivanov E, Todorov P, Petrova I, Volynets N, Paddubskaya A, Kuzhir P, Uglov V, Biró I, Kertész K, Márk GI, Biró LP:Mechanical and electromagnetic properties of 3D printed hot pressed nanocarbon/poly(lactic) acid thin films, J. Appl. Phys. 121 (2017) 064105.
[35] Lamberti P, Spinelli G, Kuzhir P, Guadagno L, Naddeo G, Romano V, Kotsilkova R, Angelova P, Georgiev V: Evaluation of thermal and electrical conductivity of carbon-based PLA nanocomposites for 3D printing, Conf. Proc. 9th Conf. on Times of Polym. (TOP) & Composites, Ischia (2018).

Applied Rheology
To appear as: Appl. Rheol. 28 (2018) 54014
DOI: 10.3933/ApplRheol-28-54014

Figure and Table Captions

Figure 1: Complex viscosity η^* versus angular frequency of: (a) MWCNT/PLA and (b) GNP/PLA nanocomposites at 200°C with varying the filler contents from 0 to 12 wt%.

Figure 2: Storage and loss moduli G' and G" versus angular frequency of: (a) MWCNT/PLA and GNP/PLA nanocomposites at 200°C with varying the filler contents from 0 to 12 wt%.

Figure 3: Cole-Cole plot of dynamic viscosity η' versus imaginary viscosity $\eta"$ for: (a) MWCNT/PLA and (b) GNP/PLA nanocomposite at 200°C with varying the filler contents of 0 - 12 wt%.

Figure 4: van Gurp–Palmen plot for GNP/PLA (left) and MWCNT/PLA (right) nanocomposites at 200°C with varying the filler contents of 0 - 12 wt%.

Figure 5: The plateau storage modulus G_o' at ω = 0.1 rad/s as a function of MWCNT and GNP loading. Arrows point the rheological percolation threshold.

Figure 6: TEM micrographs of the cross section of filament produced from: (a, c) MWCNT/PLA and (b, d) GNP/PLA nanocomposites at 6 wt% filler contents at high and low magnifications.

Figure 7: Flow curves for: (a) GNP/PLA and (b) MWCNT/PLA nanocomposites at 200°C with varying filler contents. Arrows show the viscosity and shear rates for the neat PLA and 12 wt% filled composites during 3D printing with volumetric flow rate of Q = 2mm/s and nozzle diameter d = 0.5 mm at T = 200°C.

Figure 8: Samples for thermal conductivity test, 3D printed by German Rep Rap X400 3D printer FDM, using filaments produced from the neat PLA, the MWCNT/PLA and GNP/PLA nanocomposites.

Table 1: Characteristics of GNPs and MWCNTs used in PLA nanocomposites.

Table 2: Relation between the index of flow n and the increase of the printing velocity of composites V_{comp} compared to the printing velocity of neat PLA V_{PLA} at fixed Q.

Table 3: Calculated flow index n, printing rate, and printing speed of the neat PLA, the MWCNT/PLA, and the GNP/PLA nanocomposites (1 = Newtonian composites, 2 = percolated composites, and 3 = elastic solids).

Applied Rheology
To appear as: Appl. Rheol. 28 (2018) 54014
DOI: 10.3933/ApplRheol-28-54014

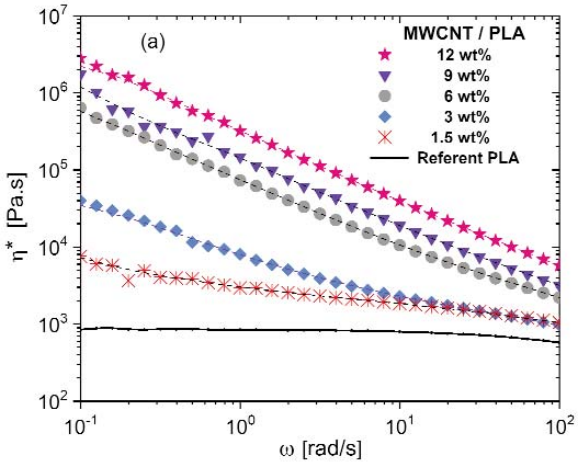

1a

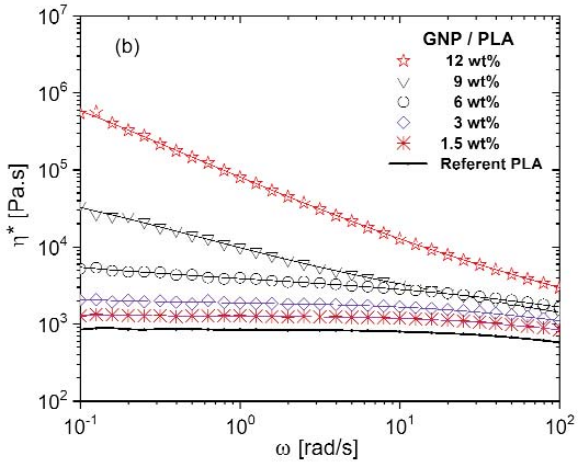

1b

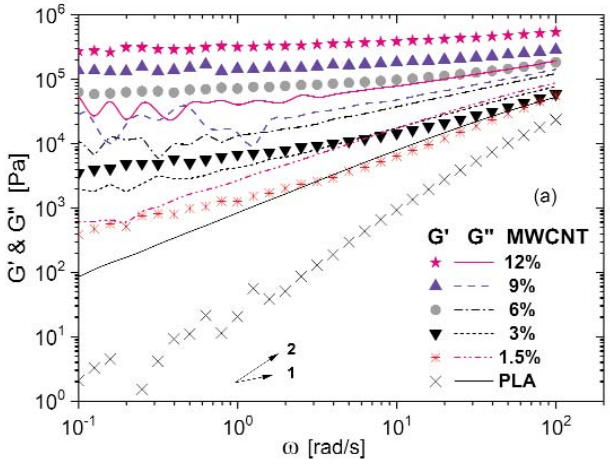

2a

Applied Rheology
To appear as: Appl. Rheol. 28 (2018) 54014
DOI: 10.3933/ApplRheol-28-54014

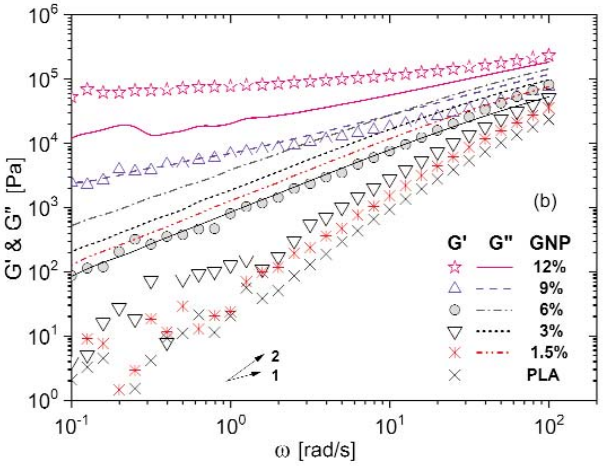

2b

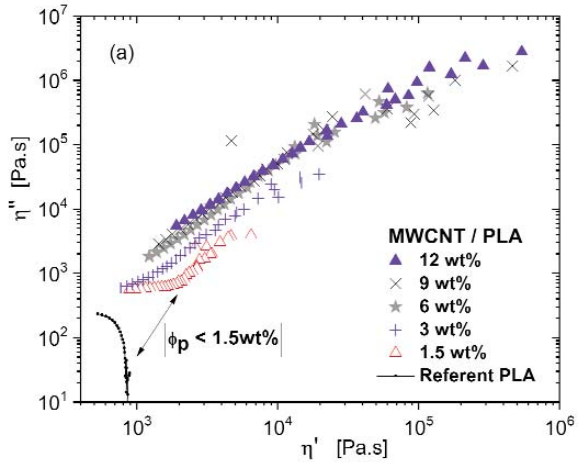

3a

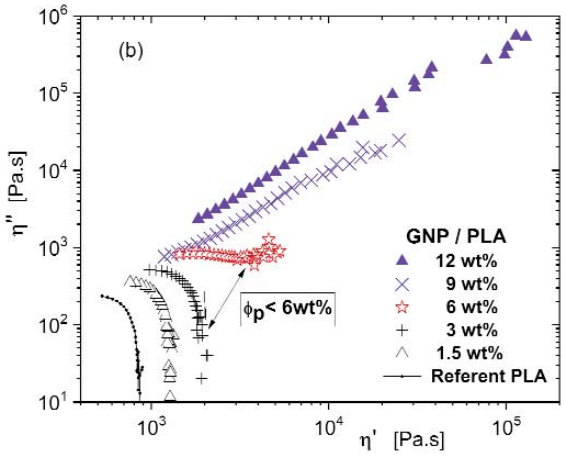

3b

Applied Rheology
To appear as: Appl. Rheol. 28 (2018) 54014
DOI: 10.3933/ApplRheol-28-54014

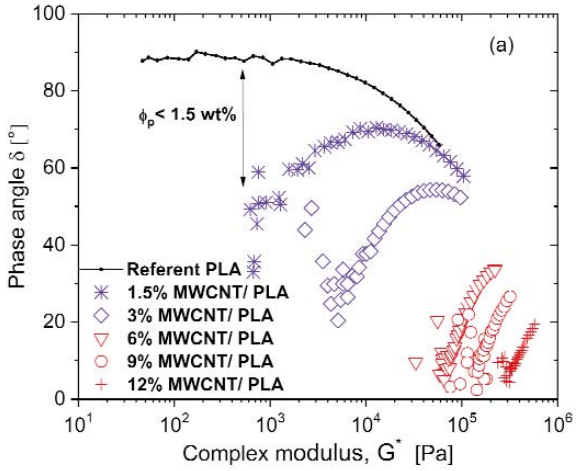

4a

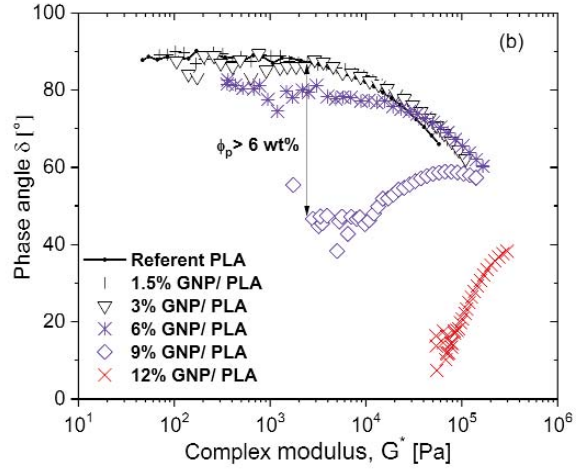

4b

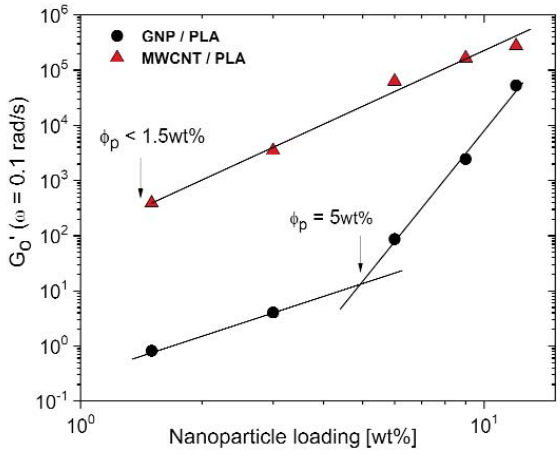

5

Applied Rheology
To appear as: Appl. Rheol. 28 (2018) 54014
DOI: 10.3933/ApplRheol-28-54014

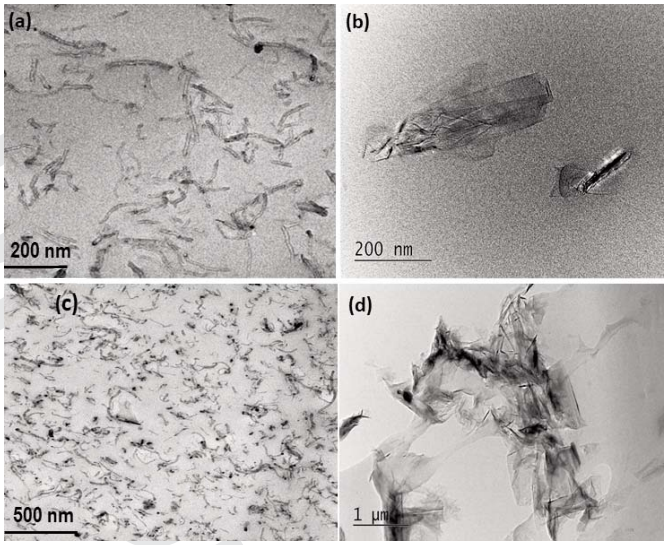

6

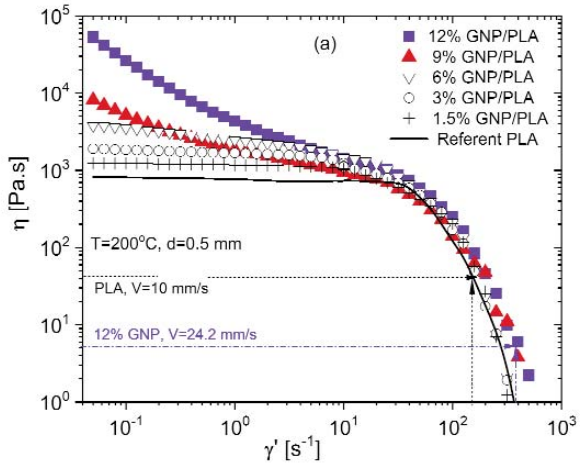

7a

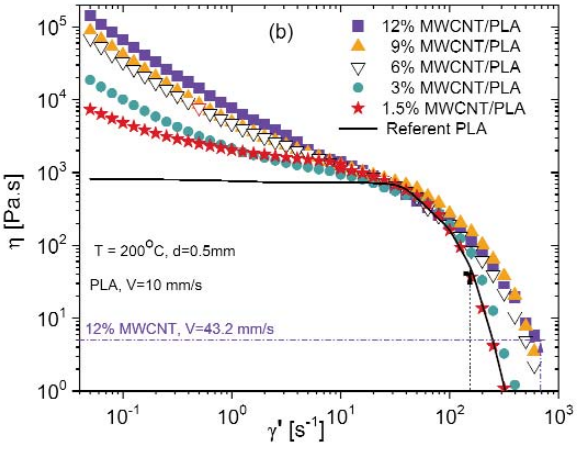

7b

Applied Rheology
To appear as: Appl. Rheol. 28 (2018) 54014
DOI: 10.3933/ApplRheol-28-54014

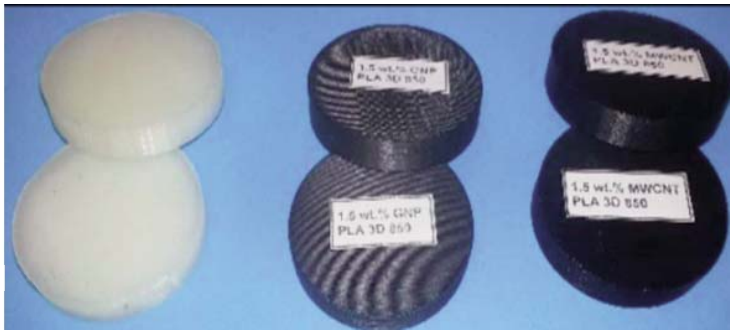

8

Property	GNPs	MWCNTs
Purity, wt.%	90	95
Number of layers / Thickness, nm	<30	-
Diameter/medium size, μm	5-7	-
Length, μm	-	10-30
Outer diameter, nm	-	10-30
Aspect ratio	~ 240	>1000
OH-content, %	-	2.48
True density, g/cm^3	2.2	2.1

1

Nanocomposite type	Filler content, ϕ, wt%	Index of flow n	Increase of V_{comp} at Q=const.
Neat PLA	$\phi = 0$	1.0	V_{PLA}
Newtonian composite	$\phi << \phi_p$	$1.0 > n > 0.5$	$(1.0 – 1.2)*V_{PLA}$
Percolated composite	$\phi \geq \phi_p$	$0.5 > n > 0.2$	$(1.3 – 2.0)*V_{PLA}$
Elastic solids	$\phi >> \phi_p$	$0.2 > n > 0.05$	$(2.1 – 6.0)*V_{PLA}$

2

Applied Rheology
To appear as: Appl. Rheol. 28 (2018) 54014
DOI: 10.3933/ApplRheol-28-54014

Filler content wt.%	Flow index, Power-law slope (n)		Printing shear rate and printing speed for Q=2 mm/s, nozzle d=0.5 mm, at T=200°C			
	MWCNT/PLA	GNP/PLA	MWCNT/PLA		GNP/PLA	
			$\dot{\gamma}$, s^{-1}	V, mm/s	$\dot{\gamma}$ [s^{-1}]	V, mm/s
0 (PLA)	1 (1)	1 (1)	160	10	160	10
1.5	0.515 (2)	0.981 (1)	198	12.4	160	10
3	0.206 (2)	0.955 (1)	314	19.6	162	10.1
6	0.137 (3)	0.813 (1)	413	25.8	170	10.6
9	0.100 (3)	0.353 (2)	520	32.5	234	14.6
12	0.070 (3)	0.150 (3)	691	43.2	392	24.2

3